Omni-directional mirror for visible light based on one-dimensional photonic crystal

Huihuan Guan (关慧欢)[1,2], Peide Han (韩培德)[1,2*], Yanqing Yang (杨艳青)[1,2], Yuping Li (李玉平)[1,2], Xue Zhang (张 雪)[1,2], and Wenting Zhang (张文婷)[1,2]

[1] *College of Materials Science and Engineering, Taiyuan University of Technology, Taiyuan 030024, China*

[2] *Key Laboratory of Interface Science and Engineering in Advanced Materials, Taiyuan University of Technology, Ministry of Education, Taiyuan 030024, China*

[*] *Corresponding author: hanpeide@tyut.edu.cn*

Received January 19, 2011; accepted March 15, 2011; posted online May 26, 2011

The omni-directional reflection characteristics of one-dimensional photonic crystals composed of Ta_2O_5/MgF_2 multi-quantum well (MQW) are studied using the transfer matrix method. An omni-directional reflector consisting of three and four Ta_2O_5/MgF_2 MQWs is investigated. Results show that the photonic band gap of the photonic crystal composed of three and four Ta_2O_5/MgF_2 MQWs, which are within the wavelength ranges of 402–712 and 412–1,023 nm, respectively, could cover the entire visible region. The relationship among the width of the band gap, its location, reflectivity rate, and incident angle of the incident light is analyzed. The optimal structural parameters of the MQW of the omni-directional reflector in the visible region are also calculated. The calculations provide a guide for the design of omni-directional reflection devices in the visible region.

OCIS codes: 160.5298, 230.4205, 310.4165, 230.4040.

doi: 10.3788/COL201109.071603.

Photonic crystal (PC) is periodic in terms of structure in the geometric scale, and in most cases, it is artificially designed and manufactured. Due to their potential value in photonic devices[1−3], including photonic filters and diodes, in visible and near-infrared regions, PCs have attracted considerable attention in recent years. However, research progress on omni-directional reflectors in this specific wave range has been insignificant due to the lack of materials suitable for the visible band, as well as the relatively narrow band gap that has been obtained. There are two types of reflectors: metallic and multilayer dielectric. Metallic reflectors can reflect light over a wide range of frequencies for arbitrary incident angles. However, at visible, optical, or higher frequencies, considerable power is lost to absorption. On the other hand, multilayer dielectric reflectors can achieve extremely low losses, and are highly reflective at certain frequency ranges.

Currently, studies on the broad band gap, omni-direction, and high reflectivity photonic band gap (PBG) incorporate two aspects. First is the selection of high and low refractive index materials, which is an outcome of the limited number of materials with high refractive index in the visible region. Consequently, the difficulty in the acquisition of appropriate refractive materials results in the broadening of the PBG in the visible region. Second is the improvement of the model, including encapsulation, identification of defects[4,5], nesting[6], and multi-quantum well (MQW)[7−10] and its adoption which has become an effective method for broadening the band gap. Recent studies have shown that a multilayer dielectric reflector can have high reflectivity over a broad range of frequencies at all incident angles or an omni-directional total reflection, if the refractive index and thickness of the constituent dielectric layers are chosen properly. For example, Wang *et al.* found that more one-dimensional (1D) PCs can be used to form multiple photonic heterostructures to obtain the desired width of omni-directional total reflection frequency range[11]. This can be achieved provided that the directional PBGs of the adjacent 1D PCs at any incident angle overlap each other in tandem. Ye *et al.* used different materials and achieved the same result, that is, a multilayer dielectric reflector could have high reflectivity over a broad range of frequencies at all incident angles[12]. The photonic quantum well facilitates designing reflectors with high reflectivity rate and omni-directional reflection which can be applied in optical fibers, waveguides, laser devices, and reflection devices[12−17].

Current studies on 1D, two-dimensional (2D), and three-dimensional (3D) PCs focus on the infrared waves, microwaves, millimeter-wave[18−20], visible light, and ultraviolet, which are short waves. Due to the limitations on material selection and preparation technology, research on omni-directional reflectors is relatively rare. PCs with 1D multilayer structure have the advantage of simplicity, ease of preparation, and low cost. Ta_2O_5 and MgF_2 are two kinds of optical materials with the appropriate proportion of high-to-low refractive index in the visible band and lower absorption.

In this letter, Ta_2O_5 and MgF_2 are selected as high and low refractive index materials, respectively. The photonic quantum well is introduced to the Ta_2O_5/MgF_2 multilayer design to achieve and broaden the omni-directional PBG in the visible region.

The structure of the 1D PC is shown in Fig. 1. The periodic structure is composed of MQW Ta_2O_5 with a high refractive index and MgF_2 with low refractive index. In Fig. 1, A, C, and E represent Ta_2O_5; B, D, and F represent MgF_2; $(AB)_m$, $(CD)_n$, and $(EF)_l$ compose of Ta_2O_5 and MgF_2, where m, n, and l com-

prise the periodic layers of a unit cell. The quantum well unit cell constant is represented as d_i, and $d_1 = d_A + d_B, d_2 = d_C + d_D, d_3 = d_E + d_F$, while $\mathbf{k}$ and f represent wave direction $\mathbf{k} = k_2\mathbf{i}_2 + k_3\mathbf{i}_3$, and its frequency f=ck/ε_0, respectively. c is the speed of light in vacuum and $\mathbf{i}_2$ and $\mathbf{i}_3$ are the wave vectors of light in the X and Z directions, respectively. The wave vector of the photonic quantum well can be divided into two polarized modes, transverse electric (TE) and transverse magnetic (TM). In the TM mode, light wave propagation is perpendicular to the electric field, whereas in the TE mode, light wave propagation is perpendicular to the magnetic field. Omni-directional reflection occurs when the position of the PBG and its width are not influenced by the incident angle in the two polarized modes.

Simulation calculation was performed with Translight software designed by the Glasgow University. The transfer matrix method was applied to study the reflective characteristics of the photonic quantum well of Ta_2O_5/MgF_2. During the calculation, the whole model system was divided into several small periodically repetitive units. The MQW was considered to be limited in the incident direction, that is, Ta_2O_5/MgF_2 was limited in the Z direction, and infinite in the X and Y directions. The general dielectric constant ε_i=ε_i'+j$\varepsilon_i'' = (n_i$+j$k_i)^2$ $(i = 1, 2)$, where n_i and k_i represent the real and imaginary parts of the refractive index, respectively, and ε_i' and ε_i'' represent the real and imaginary parts of the dielectric constant, respectively. Figure 2 shows the adopted refractive indices of Ta_2O_5 and MgF_2, indicating that the two imaginary parts of the refractive indices of Ta_2O_5 and MgF_2 are approximately zero in the visible band, and the imaginary part of the dielectric constant is approximately zero. Therefore, the visible light absorption of the photonic quantum well is negligible in this letter. During the calculation, only the real part, $\varepsilon_i' = n_i^2$, was selected as the dielectric constant.

The reflectivity rates of the three MQW, $(AB)_m$, $(CD)_n$, and $(EF)_l$ were calculated first through the simulation, where the periodic layer of Ta_2O_5/MgF_2 was 6, the thickness ratio of Ta_2O_5 to MgF_2 remained constant at 2:3, and the thickness was $d_A = 74$ nm, $d_B = 111$ nm, $d_C = 62$ nm, $d_D = 93$ nm, $d_E = 54$ nm, and $d_F = 81$ nm. Figures 3(a)–(c) show the reflectivity curve of $(AB)_m$, $(CD)_n$, and $(EF)_l$, respectively. A PBG is visible in a single quantum well. However, the band gap width is generally narrow. It is located at 547–709, 459–594, and 400–518 nm, respectively. A comparison of the PBGs of the three quantum wells show that the gaps could overlap, and the visible light (400–709 nm) would be covered.

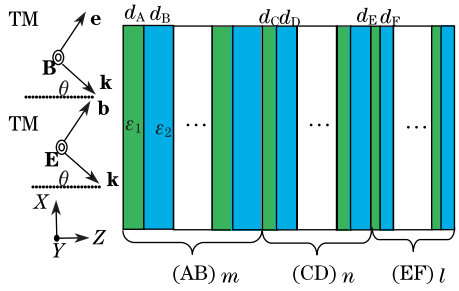

Fig. 1. 1D photonic quantum well structure model, in which ε_i and d are the dielectric constant and thickness, $\mathbf{k}$, $\mathbf{E}$, and $\mathbf{B}$ are the wave vector, electric, and magnetic fields, respectively.

Therefore, the combined MQW of $(AB)_m$, $(CD)_n$, and $(EF)_l$ was analyzed. Figure 3(d) shows significant increase in the PBG width and the formation of the PBG in the range of 402–712 nm, which covered the overlapping area of the three PBGs in the quantum wells $(AB)_m$, $(CD)_n$, and $(EF)_l$. Thus, the application of MQW could broaden the width of the PBG effectively. However, Fig. 3(d) indicates that the reflectivity rate obtained with these specific structural parameters failed to reach 100%.

To analyze the influence of the periodic layer on the reflection characteristics of MQW, the analysis was conducted when the MQW periodic layers of $(AB)_m/(CD)_n/(EF)_l$ was $m = n = l = 6$, 8, and 10, respectively, as shown in Fig. 4. In Fig. 4(a), $m = n = l = 6$, whereas in Figs. 4(b) and (c), $m = n = l = 8$ and 10, respectively. Figure 4 indicates that under the condition of normal incidence, the reflection curve gradually becomes smooth with the increase of repetitive periodic layers. When the periodic layer reached 10, the PBG was located at the 392–712 nm wave and covered the visible region completely, with the reflection rate reaching approximately 100%.

In order to study the omni-directional reflection characteristics of Ta_2O_5/MgF_2 MQW, the analysis on reflection characteristics of the PBG formed in MQW was

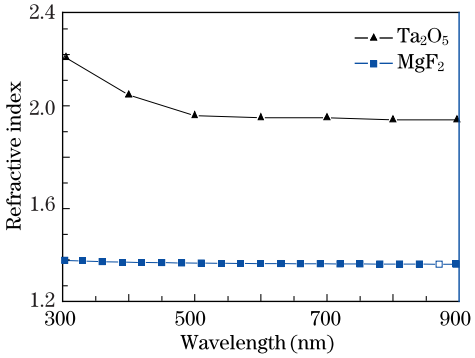

Fig. 2. Refractive indices of Ta_2O_5 and MgF_2 as a function of wavelength.

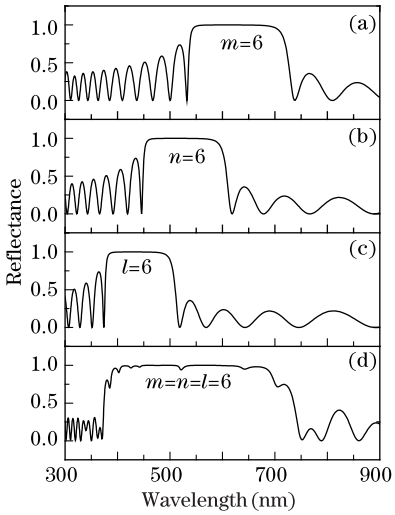

Fig. 3. Reflectance spectra for (a) $(AB)_6$, (b) $(CD)_6$, (c) $(EF)_6$, and (d) $(AB)_6/(CD)_6/(EF)_6$ photonic quantum well structure.

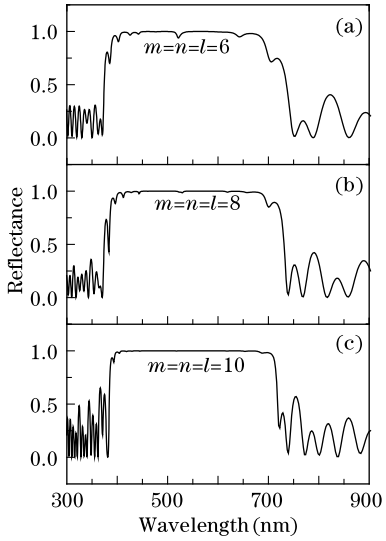

Fig. 4. Effect of different periodic layers on the reflectance spectra of the $(AB)_m/(CD)_n/(EF)_l$ photonic quantum well structure.

conducted using different incident angles. The reflection spectra of the TM and TE modes are shown in Figs. 5(a) and (b), respectively. When the angle between the incident light wave vector and Z direction is 0°, the PBGs in the TE and TM modes completely overlapped. Figure 5(a) shows that the increase of the incident angle facilitats the movement of the initial and terminal positions of band gaps to a shorter band, called blue shift, and the change of the TM mode is significantly enhanced compared with that of the TE mode. In the two polarized modes, the band gap position and the reflectivity rate are stable at the deflection angle of 0°–30°. However, when the deflection angle is between 30° and 90°, the occurrence of blue shifting of the band gap is significant, and the gap width in the TM mode becomes narrower. Figure 5 shows the band gap overlap in the TE and TM modes, when the deflection angle is between 0° and 90°. Results indicate that the structure in the wavelength range of 403–530 nm has reflection characteristics. However, the omni-directional reflection band gap did not fully cover the entire visible band. Therefore, the reflection characteristics of the combined structure of the four quantum wells were studied.

The reflection spectra of the four multi-layer structures of MQW $(AB)_m$, $(CD)_n$, $(EF)_l$, and $(MN)_s$ are shown in Fig. 6. The periodic layer of Ta_2O_5/ MgF_2 is 6, the thickness ratio is 2:3, and thicknesses are $d_A = 104$ nm, $d_B = 162$ nm, $d_C = 86$ nm, $d_D = 129$ nm, $d_E = 68$ nm, $d_F = 102$ nm, $d_M = 68$ nm, and $d_N = 181$ nm. The reflectivity curves of quantum wells $(AB)_m$, $(CD)_n$, $(EF)_l$, and $(MN)_s$ are shown in Figs. 6(a)–(d), respectively, corresponding to the location of the PBG at 799–1034, 635–824, 503–652, and 400–518 nm. Similarly, the PBGs of four combined MQWs are analyzed. Figure 6(e) shows that the PBG of the four combined quantum wells is between 402 and 1,050 nm, covering both visible light and near-infrared band. In Fig. 6(e), the reflectivity near 700 nm did not reach 100%. The effect of the periodic layers was also analyzed. The reflection spectra of MQW $(AB)_m/(CD)_n/(EF)_l/(MN)_s$ are shown in

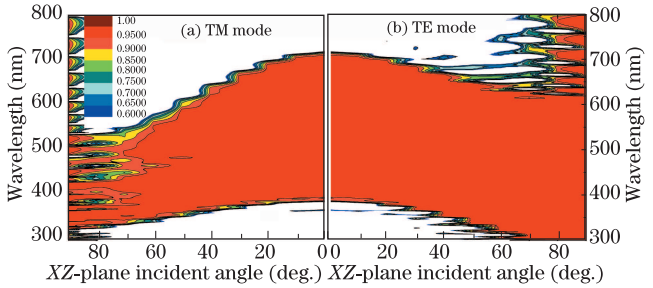

Fig. 5. Effect of different incident angles on the photonic band gap position of the multi-quantum-well structure $(AB)_{10}/(CD)_{10}/(EF)_{10}$ in the (a) TM and (b) TE modes.

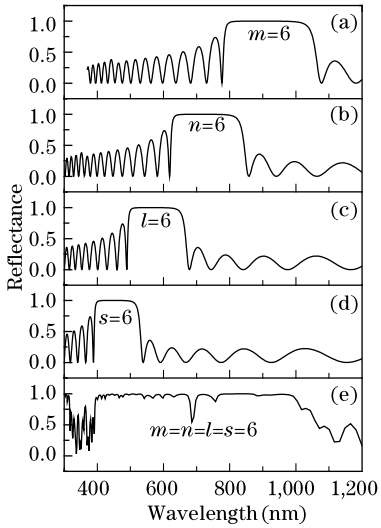

Fig. 6. Reflectance spectra for (a) $(AB)_6$, (b) $(CD)_6$, (c) $(EF)_6$, (d) $(MN)_6$, and (e) $(AB)_6/(CD)_6/(EF)_6/(MN)_6$ photonic quantum well structure.

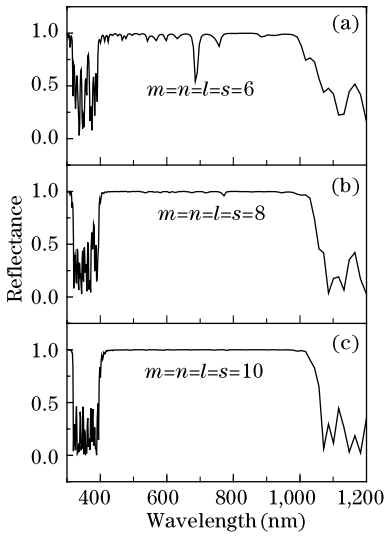

Fig. 7. Influence for the reflectance spectra of $(AB)_m/(CD)_n/(EF)_l/(MN)_s$ photonic quantum well structure.

Fig. 7, and the periodic layer is $m = n = l = s = 6$, 8, and 10. Under the condition of normal incidence, the reflection curve became smoother with the increase of the periodic layer. When the periodic layer reached 8, the PBG was located at the wave band of 412–1,023 nm,

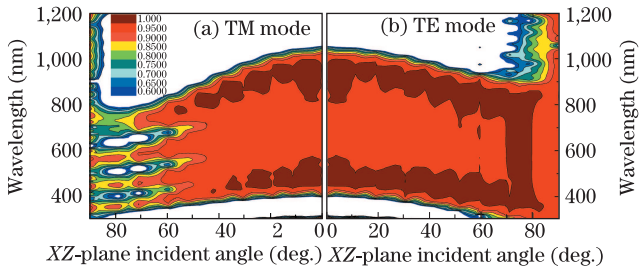

Fig. 8. Effect of different incident angles on the photonic band gap position of the multi-quantum-well structure with the layers of cycle structures $(AB)_m/(CD)_n/(EF)_l/(MN)_s$ in the (a) TM and (b) TE modes.

covering the visible and near-infrared region completely, with the reflectivity rate at approximate 100%.

Figure 8 shows the influence curve of the incident angle affecting omni-directional reflectivity characteristics. The influence of incident angle on PBGs in MQW is similar to that in Fig. 5. The reflection spectra of the TM and TE modes are shown in Figs. 8(a) and (b), respectively. The occurrence of the blue shift of the band gap with the increase of the incident angle is more significant in the TM mode than in the TE mode. With the change in deflection angle from 0° to 90°, the overlapping of band gaps in the two polarized modes existed at the 414–771 nm wavelength band, covering the entire visible region. Thus, the omni-directional reflector is achieved in the visible region.

In conclusion, the transfer matrix method is used to study the omni-directional reflection characteristics of 1D PC composed of Ta_2O_5/MgF_2 MQW in the visible region. The results reveal that the PBGs of three and four Ta_2O_5/MgF_2 MQWs are located at the 402–712 and 412–1,023 nm bands, respectively. When the periodic layer of each quantum well reaches the eighth layer, the omni-directional reflector, formed by the combination of four Ta_2O_5/MgF_2 MQWs, covers the entire visible region completely. Hence, the results of this study can provide guidance in the design of an omni-directional reflector in the visible region, as well as of the design of solar cells.

This work was supported by the National Natural Science Foundation of China (No. 50874079), the Natural Science Foundation of Shanxi Province (No. 2006011053), and the Taiyuan Science and Technology Project (No. 100115105).

References

1. T. Murzina, F. Y. Sychev, E. Kim, E. Rau, S. Obydena, O. Aktsipetrov, M. Bader, and G. Marowsky, J. Appl. Phys. **98,** 123702 (2005).
2. V. N. Belyi, N. S. Kazak, S. N. Kurilkina, and N. A. Khilo, Opt. Commun. **282,** 1998 (2009).
3. G. H. Rui, Y. H. Lu, P. Wang, H. Ming, and Q. W. Zhan, Opt. Commun. **283,** 2272 (2010).
4. Q. Ji, X. Ma, J. Sun, H. Zhang, and Y. Yao, Chin. Opt. Lett. **8,** 398 (2010).
5. X. Li, K. Xie, and H.-M. Jiang, Opt. Commun. **282,** 4292 (2009).
6. N. Ansari, M. M. Tehranchi, and M. Ghanaatshoar, Phys. B **404,** 1181 (2009).
7. Y. Han and K. Xie, Acta Photon. Sin. (in Chinese) **37,** 1391 (2008).
8. S. Xu, X. Ding, Z. Xiong, Y. Liu, Y. Liu, Z. Wang, J. Zi, and X. Hou, Photon. Nanostruct. **4,** 17 (2006).
9. S. Xu, Z. Xiong, L. Gu, Y. Liu, X. Ding, J. Zi, and X. Hou, Solid State Commun. **126,** 125 (2003).
10. H. Qiang, L. Jiang, and X. Li, Opt. Laser Technol. **42,** 105 (2010).
11. X. Wang, X. Hu, Y. Li, W. Jia, C. Xu, X. Liu, and J. Zi, Appl. Phys. Lett. **80,** 4291 (2002).
12. H. Ye and G. Chen, Acta Photon. Sin. (in Chinese) **34,** 1245 (2005).
13. H. Inouye, M. Arakawa, J. Ye, T. Hattori, H. Nakatsuka, and K. Hirao, IEEE J. Quantum Electron. **38,** 867 (2002).
14. S. K. Srivastava, S. K. Awasthi, S. K. Srivastava, and S. P. Ojha, Optoelectron. Lett. **6,** 1 (2010).
15. P. J. Yao, X. Y. Chen, B. Chen, Y. H. Lu, P. Wang, X. J. Jiao, H. Ming, and J. P. Xie, Opt. Commun. **236,** 101 (2004).
16. H. Y. Lee and T. Yao, J. Appl. Phys. **93,** 819 (2003).
17. K. B. Crozier, V. Lousse, O. Kilic, S. Kim, S. H. Fan, and O. Solgaard, Phys. Rev. B **73,** 115126 (2006).
18. H. B. Lin, R. J. Tonucci, and A. J. Campillo, Opt. Lett. **23,** 94 (1998).
19. I. Nusinsky and A. A. Hardy, J. Opt. Soc. Am. B **27,** 2731 (2010).
20. S. Dang, Opt. Rev. **15,** 255 (2008).